Published in final edited form as:
Am J Physiol Endocrinol Metab. 2008 June ; 294(6): E1178–E1186. doi:10.1152/ajpendo.90237.2008.

Differential modulation of L-type calcium channel subunits by oleate

Yingrao Tian[1,2], **Richard F. Corkey**[2], **Gordon C. Yaney**[2], **Paula B. Goforth**[1], **Leslie S. Satin**[1], and **Lina Moitoso de Vargas**[2]

1*Department of Pharmacology and Toxicology, Virginia Commonwealth University Medical Center, Richmond, Virginia*

2*Division of Molecular Medicine and Obesity Research Center, Boston Medical Center, Boston, Massachusetts*

Abstract

Nonesterified fatty acids such as oleate and palmitate acutely potentiate insulin secretion from pancreatic islets in a glucose-dependent manner. In addition, recent studies show that fatty acids elevate intracellular free Ca^{2+} and increase voltage-gated Ca^{2+} current in mouse β-cells, although the mechanisms involved are poorly understood. Here we utilized a heterologous system to express subunit-defined voltage-dependent L-type Ca^{2+} channels (LTCC) and demonstrate that β-cell calcium may increase in part from an interaction between fatty acid and specific calcium channel subunits. Distinct functional LTCC were assembled in both COS-7 and HEK-293 cells by expressing either one of the EYFP-tagged L-type α_1-subunits (β-cell Cav1.3 or lung Cav1.2) and ERFP-tagged islet β-subunits ($i\beta_{2a}$ or $i\beta_3$). In COS-7 cells, elevations in intracellular Ca^{2+} mediated by LTCC were enhanced by an oleate-BSA complex. To extend these findings, Ca^{2+} current was measured in LTCC-expressing HEK-293 cells that revealed an increase in peak Ca^{2+} current within 2 min after addition of the oleate complex, with maximal potentiation occurring at voltages <0 mV. Both Cav1.3 and Cav1.2 were modulated by oleate, and the presence of different auxiliary β-subunits resulted in differential augmentation. The potentiating effect of oleate on Cav1.2 was abolished by the pretreatment of cells with triacsin C, suggesting that long-chain CoA synthesis is necessary for Ca^{2+} channel modulation. These results show for the first time that two L-type Ca^{2+} channels expressed in β-cells (Cav1.3 and Cav1.2) appear to be targeted by nonesterified fatty acids. This effect may account in part for the acute potentiation of glucose-dependent insulin secretion by fatty acids.

Keywords

β-cell calcium; free fatty acids; insulin secretion

During the last decade, the rise in the incidence of type 2 diabetes has occurred concomitant with epidemic obesity (20,39). The relationship between diabetes and obesity is now established, as the two disorders share common features, including insulin resistance, hypercholesterolemia, and hypertri-glyceridemia or increased plasma levels of free fatty acids (FFAs) (6,19,21,51). Several human studies show that elevation of circulating FFA levels leads to an increase of peripheral insulin resistance in a dose-dependent manner in both obese nondiabetics and type 2 diabetics (7,53,57). Moreover, obese individuals show insulin

Address for reprint requests and other correspondence: L. Moitoso de Vargas, Div. of Molecular Medicine and Obesity Research Center, Boston Medical Center, Boston, MA 02118 (e-mail: Lina.MoitosodeVargas@bmc.org).

resistance and are at high risk for diabetes; most eventually become diabetic. In addition, several studies show that obesity and insulin resistance usually precede the development of diabetes (7,12,22). Therefore, it has been proposed that diabetes is both a lipid disorder and a disease of glucose intolerance and that a converging metabolic signal may be a link between diabetes and obesity (46).

Despite the relationship between obesity and diabetes, several reports demonstrate that lipid-derived signals are actually necessary for normal insulin secretion (34,62) and advance the idea that long-chain CoA, malonyl-CoA (47), and diacylglycerol (1,15) might fulfill this requirement. The most direct evidence comes from studies showing that short-term exposure of pancreatic islets (11,48,64) or insulin-secreting cells (18) to FFA potentiates glucose-stimulated insulin secretion (GSIS).

Elevation of intracellular Ca^{2+} through voltage-dependent calcium channels (VDCC) has long been established as an important and necessary signal for GSIS from pancreatic β-cells (2,8, 33,45,55,56,66). Although many types of VDCC are expressed in pancreatic β-cells, L-type VDCC (LTCC) have emerged as major participants in insulin secretion (16,32,36,40,58). Several studies indicate that FFA modulate LTCC in different cell types (38,65), including pancreatic mouse β-cells (64) and enteroendocrine cells (38,60). FFA induces an increase in intracellular free Ca^{2+} concentration ($[Ca^{2+}]_i$), possibly as a result of increased calcium influx through LTCC, and it has been shown that palmitate increases whole cell Ca^{2+} currents solely via LTCC activation in both β- and α-cells of pancreatic mouse islets (3,42). In addition, our own work in INS-1 cells shows that exogenous oleate increases intracellular Ca^{2+} following cell depolarization and potentiates whole cell Ca^{2+} currents (Yaney GC, Moitoso de Vargas L, and Satin LS, unpublished observations). The FFA-mediated effect in $[Ca^{2+}]_i$ parallels the acute FFA-induced potentiation of GSIS, reflecting a similar glucose-dependent membrane depolarization.

Here we transiently transfected COS-7 and HEK-293 cells with different combinations of Ca^{2+} channel subunits to investigate the role of individual LTCC subunits as potential oleate targets. Our data show that in COS-7 cells oleate enhanced the amplitude of LTCC-dependent elevations in $[Ca^{2+}]_i$. In addition, in LTCC-expressing HEK-293 cells, the whole cell patch clamp technique revealed that oleate acutely increased peak Ca^{2+} current. The potentiation was voltage-dependent and was blocked by the inhibition of long-chain acyl-CoA formation. Moreover, although both LTCC α-subunits, Cav1.3 and Cav1.2, were potentiated by oleate, β-subunits imparted an additional level of regulation on this effect in Cav1.2-containing channel multimers. The results are discussed with regard to the potentiating actions of fatty acids on glucose-dependent insulin secretion in pancreatic islets of Langerhans.

MATERIALS AND METHODS

Construction and preparation of plasmids and recombinant adenovirus

Plasmids pEYFP-α_{1C} and pEYFP-α_{1D} were constructed using standard molecular biology protocols by inserting the DNA coding for the rabbit lung α_{1C} (Cav1.2) (5) or the HIT-T15 long COOH-terminal α_{1D} (Cav1.3) isoform (Moitoso de Vargas L, unpublished observations) into pEYFPC1 (Clontech) to generate in-frame fusions between the amino terminus of α_{1C} and α_{1D} and the carboxyl end of the yellow variant of the green fluorescent from *Aequora Victoria* (EYFP; Clontech), EYFP-α_{1C}, and EYFP-α_{1D}, respectively. Similarly, we generated piβ_{2a}-ERFP, pmutiβ_{2a}-ERFP, and piβ_3-ERFP to produce functional fusion proteins at the COOH-terminal end of each islet β-subunit and the amino terminus of the enhanced JRed protein (ERFP; Evrogen). Constructs were confirmed by restriction enzyme and DNA-sequencing analyses of relevant regions.

Recombinant, replication-deficient type 2 adenoviruses (rAd) containing either iβ_{2a}-ERFP, mutiβ_{2a}-ERFP, or iβ_3-ERFP at the viral E1 region were produced using the two-cosmid system (63). Briefly, the genes coding for either iβ_{2a}-ERFP, mutiβ_{2a}-ERFP, or iβ_3-ERFP were subcloned into an adenoviral shuttle vector, pLEPMV6, a pLEP (63) derivative containing the cytomegalovirus promoter and an SV40 poly(A) signal (Moitoso de Vargas L, unpublished observations) from which genomic adenoviral cosmids were subsequently obtained. rAd-expressing iβ_{2a}-ERFP, mutiβ_{2a}-ERFP, or iβ_3-ERFP (Ad iβ_{2a}-ERFP, Ad mutiβ_{2a}-ERFP, or Adiβ_3-ERFP, respectively) were generated by transfecting HEK-293 cells with the isolated adenoviral cosmid. The correct DNA inserts were verified and confirmed in the rAd genome by polymerase chain reaction and restriction enzyme analyses, and protein expression was demonstrated by imaging of iβ_{2a}-ERFP, mutiβ_{2a}-ERFP, or iβ_3-ERFP-transduced COS-7 cells prior to viral amplification and CsCl purification as described (17).

Transduction/transfection of COS-7 cells

COS-7 and HEK-293 cells were acquired from American Type Culture Collection and grown using standard protocols. COS-7 cells cultured in DMEM containing 10% FBS and 1% penicillin-streptomycin were plated into 35-mm poly-D-lysine-coated glass bottom microwell dishes (MatTek) at ~0.5×10^5/ml. Following overnight culture, cells were treated with virus (Ad iβ_{2a}-ERFP, Ad mutiβ_{2a}-ERFP, or Ad iβ_3-ERFP) at a multiplicity of infection of $1–5 \times 10^{2–4}$ particles/cell for 1 h at 37°C, followed by transient transfection of 1 mg of plasmid DNA (pEYFP-α_{1C} or pEYFP-α_{1D}) using FuGENE 6 (Roche) according to the manufacturers' instructions. After 3 h at 37°C, more DMEM medium was added and the cells were further incubated for 48 h. COS-7 passage number was not found to affect the expression of VDCC subunits, an observation that was also verified in HEK-293 cells.

Fura 2 loading and measurements of Ca^{2+}

Fura 2-AM (Molecular Probes) was used for ratiometric measurement of $[Ca^{2+}]_i$ values using excitation at 340 and 380 nm and emission at 510 nm, as described previously (27). Briefly, Ca^{2+} measurements from single LTCC-expressing or control COS-7 cells were carried out after cells were loaded for 90 min at 37°C in the presence of 0.2% pluronic F-127 (Molecular Probes) with fura 2-AM (2 μM) in Krebs-Ringer-bicarbonate buffer containing 10 mM glucose, 2 mM $CaCl_2$, and 0.05% BSA. After loading, the cells were washed, incubated in the same buffer without pluronic for 15 min, and imaged to select yellow fluorescent protein (YFP)- and red fluorescent protein (RFP)-expressing cells using a Zeiss IM 35 inverted microscope and a ×40 glycerin objective in a temperature-controlled cabinet heated to 37°C. A xenon lamp and a dual-excitation filter (51019 series) from Chroma were used to excite YFP and RFP differentially. A dual dichroic and emission filter pair from the same series (Chroma) allowed the selective imaging of YFP and RFP. Subsequently, intracellular fura 2 of selected cells was excited at 340 and 380 nm and emission signals (510 nm) recorded by a charge-intensified charge-coupled device camera. Images were collected at 8-s intervals. Data were acquired and analyzed using IonWizard software (IonOptix). The free Ca^{2+} concentration was calculated from the fluorescence ratio (25). A K_d of 224 nm/l for Ca^{2+} binding to free fura 2 was used in calculations.

Preparation of BSA-oleate complexes

An oleate-BSA complex was used, since most long-chain fatty acids in the circulation are bound to albumin with a free FFA concentration ranging from 0.01 to 10 μM (61). A complex of 20 mM oleate was made as follows. A 35% BSA stock was prepared in dH_2O by very slowly adding fatty acid-free BSA (Sigma) in small aliquots with minimal stirring. The final concentration of BSA was determined by the solution's absorbance at 280 nm minus that at 350 nm and assuming a molecular weight of 67,000. A 50-mM oleate stock was prepared in 4

mM NaOH using the sodium salt of oleate (Sigma). Combining 1 ml of 50 mM oleate stock and 1.5 ml of 4 mM BSA after heating both to 55°C results in 2.5 ml of 20 mM oleate at an oleate/BSA ratio of ~8.3:1. Because BSA has multiple binding sites for FFA, this FFA/oleate ratio provides an estimated concentration of 0.5% of free oleate in the oleate-BSA complex (52). The different oleate concentrations in the experiments reported here thus approximate the in vivo levels of unbound FFA.

Culture and transfection of HEK-293 cells

HEK-293 cells were placed on glass coverslips in 35-mm petri dishes and cultured in MEM medium with 10% FBS, 1% L-glutamine, and 1% penicillin-streptomycin. Cultures were kept at 37°C in an air-5% CO_2 incubator. Cells were transiently transfected by the calcium phosphate precipitation method 30 h after plating using 0.5 μg of each construct. Following transfection, cells were washed with PBS for 10 min, which was then replaced with fresh medium supplemented with 10 mM $MgCl_2$.

Electrophysiology

Twenty-four hours after transfection, HEK cells were visually selected for recording by yellow fluorescent protein fluorescence. Whole cell or perforated patch clamp recordings were performed with an Axopatch 1-D amplifier (Axon Instruments). Patch pipettes (4–6 Mohm) contained 114 mM Cs aspartate, 10 mM $CsCl_2$, 4 mM Mg_2ATP, 10 mM HEPES, and 1 mM EGTA with or without 0.15 mg/ml amphotericin B (pH 7.2). The extracellular recording solution contained 115 mM NaCl, 3 mM $CaCl_2$, 5 mM $CsCl_2$, 1 mM $MgCl_2$, 10 mM HEPES, 11.1 mM glucose, and 0.05% BSA (pH 7.2). In a small subset of cells, $CaCl_2$ was replaced by 3 mM $BaCl_2$, which did not affect the degree of current potentiation by oleate. Recordings were performed at a holding potential of −65 mV, and peak current was acquired at 0 mV unless otherwise indicated in the text.

Data analysis

Unless otherwise stated, data analysis and graphics were implemented using IGOR Pro software, and statistics were performed using Prism3 software. Data are presented as means ± SE for the indicated number of experiments. Statistical significance between two means was evaluated using Student's *t*-test.

RESULTS

Effect of oleate in $[Ca^{2+}]_i$ of Cav1.3 or Cav1.2 plus $i\beta_{2a}$–-expressing COS-7 cells

We established a heterologous system (COS-7 cells) to express differentially fluorescent-labeled α_1- and β-subunit isoforms of L-type VDCC and performed intracellular $[Ca^{2+}]$ measurements of fura 2-loaded single cells according to the procedures described in MATERIALS AND METHODS. A similar protocol has been described previously and validated (37). Parallel control experiments were performed with COS-7 cells lacking transgenes or expressing only one of the VDCC subunits (either EYFP-α_1 or β_{2a}-ERFP alone). The resting membrane potential of COS-7 cells, −31 mV, is comparable with that evoked by 7 mM glucose in native β-cells and which supports tonic activation of the Cav1.3-containing channel (67).

Under these conditions, an increase in extracellular $[Ca^{2+}]$ would be expected to cause a concomitant rise in intracellular $[Ca^{2+}]$ in COS-7 cells expressing functional Cav1.3-$i\beta_{2a}$ Ca^{2+} channels. Intracellular $[Ca^{2+}]$ was measured in single fura-2 loaded COS-7 cells under conditions of 2 mM (basal) or 5 mM extracellular Ca^{2+} and in the presence or absence of the oleate-BSA complex. The dependence of the Ca^{2+} changes observed in VDCC was confirmed

using the L-type Ca^{2+} channel agonist Bay K 8644, and the viability and integrity of control COS-7 cells were confirmed with 10 μM ATP, which releases intracellular Ca^{2+} from internal stores (4).

Compared with control COS-7 cells, on average, $[Ca^{2+}]_i$ in Cav1.3-iβ_{2a}-expressing COS-7 cells was elevated by 40% when bathed in 2 mM (basal) extracellular Ca^{2+}. Also, as shown in Fig. 1*A*, increasing extracellular Ca^{2+} to 5 mM ($CaCl_2$) resulted in a rise in intracellular $[Ca^{2+}]$ in Cav1.3-iβ_{2a}-expressing COS-7 cells, but not in COS-7 lacking heterologously expressed LTCC subunits (Fig. 1*B*) or in those with iβ_{2a} only (data not shown). Moreover, subsequent addition of the oleate complex further increased intracellular Ca^{2+} in Cav1.3-iβ_{2a}-expressing COS-7 cells, but not in control cells lacking channel expression. Oleate increased $[Ca^{2+}]_i$ by a mean of 41%, which took place within 2–8 min after its addition.

To determine whether the oleate-induced effect was restricted to Cav1.3-iβ_{2a}, the studies were extended to the Cav1.2-iβ_{2a} channel. We found that Cav1.2-iβ_{2a} channels were functionally expressed in the COS-7 heterologous system and that the activity of these channels was also subject to enhancement by oleate (Fig. 3). Oleate in this case increased $[Ca^{2+}]_i$ by a mean of 107% 1.5 min after being added.

Effect of oleate on $[Ca^{2+}]_i$ in Cav1.3 or Cav1.2 plus mut iβ_{2a}-expressing COS-7 cells

Previous work has shown that the NH_2-terminal cysteines (C3, C4) of rat brain β_{2a} undergo palmitoylation, which confers distinct properties to the LTCC that result from its association with the α_1-subunit. In particular, palmitoylation allows membrane localization and targeting of the β-subunit independently of its association with α_1, shifts its voltage activation to more negative membrane potentials, affects prepulse facilitation and channel inactivation kinetics, and results in an increase in Ca^{2+} current amplitude (13,24,29,41,49). Sequencing of the DNA coding for the rat islet β_2-isoform (iβ_{2a}) shows that, with the exception of a shortened domain III, it is identical to that of the brain β_{2a}, including domain I, and that when it is expressed alone in a heterologous system (COS-7 cells), it localizes to the plasma membrane (Moitoso de Vargas L, unpublished observations).

To test whether acylation of the two NH_2-terminal cysteines in iβ_{2a} might underlie oleate-mediated enhancement of $[Ca^{2+}]_i$ in LTCC-expressing COS-7 cells, we used site-direct mutagenesis to alter C3 and C4 to S3 and S4. The resulting mutant was then evaluated for its ability to support an oleate-induced rise in $[Ca^{2+}]_i$ in COS-7 cells expressing Cav1.2 or Cav1.3 coex-pressed with mut iβ_{2a}. The results revealed that acylation of C3 and C4 does not appear to be needed for oleate potentiation of L-type Ca^{2+} channels, because the mutations did not interfere with the action of oleate (Fig. 2*A* and Fig. 3). Thus, oleate increased $[Ca^{2+}]_i$ by a mean of 26% for Cav1.2-mut iβ_{2a}-expressing cells and 45% for Cav1.3-mut iβ_{2a}-expressing cells.

Effect of oleate on $[Ca^{2+}]_i$ in Cav1.3 or Cav1.2 plus iβ_3-expressing COS-7 cells

To ascertain the independent role of iβ_{2a} and iβ_3 (the predominant β-subunits expressed in β-cells) (31,44,68) in the fatty acid-mediated potentiation of intracellular Ca^{2+}, we independently expressed either type of α_1-subunit with rat iβ_3 (sequencing of its coding DNA revealed that it was identical to brain β_3; Moitoso de Vargas L, unpublished observations). The activation of Cav1.2 with iβ_3 in COS-7 cells, monitored as an increase in intracellular $[Ca^{2+}]$, required depolarization of the cell's membrane potential by KCl addition, reflecting the higher voltage threshold of this channel (67). The HIT T15 Cav1.3 isoform and iβ_3 combination under the experimental conditions used here, although not previously documented, also required KCl depolarization. In both cases, oleate still induced an LTCC-dependent rise in $[Ca^{2+}]_i$ in COS-7 cells (Fig. 2*B* and Fig. 3) with a mean increase of 58% for Cav1.2-iβ_3-expressing cells and

39% for Cav1.3-iβ_3-expressing cells. COS-7 cells expressing Cav1.3-iβ_3 tended to have a low signal-to-noise ratio.

Thus, under the conditions used here, only those COS-7 cells in which a functional LTCC was expressed exhibited a $[Ca^{2+}]_i$ rise, which then could be further increased upon the addition of oleate. Qualitatively, the oleate-mediated effect appeared to persist despite changes in subunit composition, although a quantitative analysis of the contribution of individual subunits was not feasible from these experiments.

Effects of oleate on Ca^{2+} current carried by calcium channels Cav1.3 or Cav1.2 plus iβ_{2a} and $\alpha_2\delta$

To verify that the oleate-mediated rise in $[Ca^{2+}]_i$ observed in LTCC-expressing COS-7 cells was the direct result of an increase in Ca^{2+} current due to FFA, and to obtain a more rigorous and quantitative analysis of the efficacy of different subunit contributions, we used a similar heterologous expression system (HEK-293 cells) to measure whole cell calcium currents in voltage-clamped HEK cells expressing Cav1.3 or Cav1.2 with iβ_{2a} and $\alpha_2\delta$ Cells were voltage-clamped to a holding potential of −65 mV, and peak inward calcium current was measured upon stepping to 0 mV. In HEK cells expressing Cav1.3, the application of 100 μM oleate-BSA increased peak Ca^{2+} current amplitude from −284 ± 54 to −318 ± 62 pA (n = 17), with a mean increase of 18.1 ± 8.3% ($P < 0.05$; Fig. 4, *A* and *B*). Of 17 cells tested, oleate increased Ca^{2+} current amplitude in 12 cells, decreased it in three, and had no effect in the remaining two cells. The effect of oleate occurred within 2 min of its addition to the bath. Similarly, application of 100 μM oleate-BSA complex increased mean calcium current amplitude in cells expressing Cav1.2 from −282 ± 54 to −324 ± 59 pA (n = 24, $P < 0.05$; Fig. 4, *C* and *D*). Of 24 cells exposed to the FA, oleate increased current amplitude in 16 cells, decreased it in five, and had no effect in the remaining three cells. The maximum potentiation occurred within 1–4 min using this subunit combination. The mean oleate-elicited increase for Cav1.2 was 23.3 ± 10.0%.

To test whether the action of oleate was voltage dependent, we constructed Ca^{2+} current-voltage (I–V) curves for HEK cells expressing Cav1.2-iβ_{2a}-$\alpha_2\delta$. Calcium currents were measured in the absence and presence of 20 or 100 μM oleate-BSA as membrane potential was changed from a standard holding potential of −65 mV to a series of potentials ranging from −70 to +50 mV. The application of 20 or 100 μM oleate increased Ca^{2+} current in a voltage-dependent manner, with the largest enhancement occurring at more negative potentials. Thus, as shown in Fig. 5*A*, 20 μM oleate increased calcium current amplitude by 111% at −30 mV, 74% at −20 mV, 54% at −10 mV, 41% at 0 mV, and 39% at +10 mV (n = 10). A similar result was obtained using 100 μM oleate, which significantly increased calcium current amplitude by 23% at −30 mV, 37% at −20 mV, 35% at −10 mV, 12% at 0 mV, and 4% at +10 mV (n = 14; data not shown). Interestingly, 20 μM oleate increased current amplitude to a greater degree than 100 μM (compare Fig. 4*B* and Fig. 5*B*).

The effect of oleate on Ca^{2+} channels possessing different β-subunits

Whole cell peak calcium currents were measured at 0 mV in HEK cells expressing either Cav1.2-iβ_{2a}-$\alpha_2\delta$ or Cav1.2-iβ_3-$\alpha_2\delta$ to test whether expression of β^{2a} vs. β_3 differentially affected oleate action. In iβ_{2a}-containing HEK cells, 20 μM oleate-BSA increased peak current amplitude from −191 ± 44 to −369 ± 82 pA (n = 9, $P < 0.01$; Fig. 5*B*), a 106 ± 21% increase. The expression of iβ_3 instead of iβ_{2a} resulted in a more modest oleate-induced current enhancement (Fig. 5, *C* and *D*). In these cells, 20 μM oleate increased calcium current at 0 mV from −241 ± 48 to −277 ± 54 pA (n = 8, $P < 0.01$), an increase of only 16 ± 2% (note that change in scales shown in Fig. 5, *B* vs. *D*).

The effect of triacsin C on oleate-regulated calcium channel Cav1.2 with $i\beta_{2a}$ and $\alpha_2\delta$

To examine the possible role of long-chain CoA synthesis in oleate-induced enhancement of calcium channels, HEK-293 cells expressing Cav1.2-$i\beta^{2a}$-$\alpha_2\delta$ were preincubated in the presence of 96 μM triacsin C (TC) for 20 min. Although not effective for all isoforms, TC is a specific and potent competitive inhibitor of acyl-CoA synthetases, the enzymes that at the plasma membrane catalyze the initial step of activating FFA to acyl-CoAs, the substrates for both synthetic and oxidative pathways (14,30). In β-cells, TC is reported to inhibit the production of long-chain CoAs (54). As shown in Fig. 6, TC treatment abolished oleate potentiation of L-type Ca^{2+} currents. After TC pretreatment, the application of 20 μM oleate had no potentiating effect on the calcium current I–V curves (Fig. 6*A*) and did not significantly increase peak calcium current measured at 0 mV, −196 ± 86 vs. −204 ± 93 pA (n = 7, not significant; Fig. 6*B*). These data suggest that long-chain CoA production is necessary for the oleate-induced increase of L-type calcium channel activity.

DISCUSSION

Previous reports indicate that short-term exposure to FFA potentiates GSIS, as well as $[Ca^{2+}]_i$, in β-cells (15,18,48). Although the molecular and cellular mechanisms underlying these effects remain elusive, it appears that the FFA increase in $[Ca^{2+}]_i$ likely involves both the influx of extracellular Ca^{2+} through LTCC as well as mobilization of Ca^{2+} from internal stores (23,59). In this study, we employed heterologous expression systems to dissect potential FFA-LTCC interactions at the level of Ca^{2+} channel subunit. Both COS-7 and HEK-293 cells were well suited for our oleate studies because neither of these cell lines expresses receptors for either long-chain (Refs. 9 and 28,Fig. 1*B*, and Demerest K and Kuo G-H, personal communication) or short-chain fatty acids (10,35). These receptors, whose tissue-specific expression was recently found, are not required for fatty acid uptake and transport because FFA readily and passively diffuse into and out of cells by the flip-flop mechanism (26). Because the two L-type calcium channels that are predominantly expressed in pancreatic β-cells, Cav1.3 and Cav1.2, are pharmacologically indistinguishable, we expressed channels of predefined subunit composition to bypass any interference from the complex LTCC expression environment of native β-cells.

Our data indicate that in COS-7 cells acute application of the oleate-BSA complex results in a $[Ca^{2+}]_i$ rise that is dependent on the functional expression of LTCC and qualitatively independent of channel subunit composition (Fig. 1–Fig. 3). Although this protocol provides a rapid and simple qualitative analysis of Ca^{2+} channel functional expression and how it may be affected by external application of compounds (e.g., acute exposure to FFA), this approach does not allow a rigorous quantitative analysis of channel biophysical properties. Thus, to verify that FFA modulates LTCC's characteristics, we expressed specific subunits of LTCC in HEK-293 cells and measured Ca^{2+} currents. We show that short-term exposure to oleate increases peak current amplitude of Cav1.3 or Cav1.2 in conjunction with either $i\beta_{2a}$ or $i\beta_3$. In our hands, the Cav1.2-β_{2a} combination was most potentiated by oleate. The heterologous expression data taken together thus support the hypothesis that increased LTCC activity in turn mediates a rise in $[Ca^{2+}]_i$. In intact β-cells, this would in turn potentiate glucose-dependen insulin granule exocytosis.

Although Cav1.3 and Cav1.2 channels exhibit similar potentiation in response to a 100-μM complex of oleate-BSA, 18 and 23%, respectively, they differ significantly in their expression rates, 15 and 80%, respectively (data not shown). For this reason, a more rigorous analysis was conducted with the latter channel. The regulation of Cav1.2 channels by oleate appears to be dose dependent, as decreasing the concentration of the oleate-BSA complex to 20 μM results in a 106% increase in current amplitude, although the time courses of the initial (2 min) and peak (15 min) responses were delayed compared with those observed with the 100-μM oleate

complex (30 s and 4 min, respectively). Analysis of the I–V curve of Cav1.2-iβ_{2a} shows that oleate regulation of these channels is voltage dependent, with a greater enhancement occurring at more negative potentials. A more detailed study of the effects of oleate on Ca^{2+} channel kinetics should further distinguish the mechanism involved.

Others have reported that palmitate exerts an effect on $[Ca^{2+}]_i$ and LTCCs in insulin-secreting cells (50,64) and increases peak current amplitude by 23% (43). However, the present study is the first to report that oleate exerts a stimulatory effect on LTCC at the subunit level. Channels with Cav1.2, $\alpha_2\delta$, and iβ_{2a} or iβ_3 all responded positively to oleate. Nevertheless, the effect of oleate on channels with iβ_{2a} (106% ± 21% increase; Fig. 5*B*) was much greater than in channels with iβ_3 (16% ± 2% increase; Fig. 5*D*), suggesting that the β-subunit plays a role in oleate regulation of channel activity. Unlike iβ_3, which does not undergo lipid-mediated posttranslational modifications, iβ_{2a} does, and an oleate-induced augmentation of the acylation status of this subunit may be the basis for the difference. Alternatively, the iβ_3 subunit may interfere with the interaction between oleate and the α_1-subunit. Thus, whereas both Cav1.3 and Cav1.2 can be modulated by oleate to a similar extent, the auxiliary β-subunit can exert further regulation of the effect. These findings may have implications for the oleate effect in β-cells, where both iβ_{2a} and iβ_3 are predominantly expressed, but their respective contributions for and associations with the Cav1.3 or Cav1.2 channels are not known. It has been reported recently that iβ_3 may not participate or even be required for LTCC activity in β-cells, but rather, it may be important for Ca^{2+} signaling involving internal Ca^{2+} stores (4).

Recent findings indicate that two components comprise the FFA-mediated Ca^{2+} increase in β-cells, mobilization from internal stores and influx through LTCC (23,59). Some authors have concluded that release from intracellular stores through activation of GPR40, a G protein-coupled receptor for medium and long-chain FFA, precedes Ca^{2+} influx through LTCC, which is dependent on GPR40-mediated Ca^{2+} release (59). The experiments reported here are not able to address the temporal sequence of this two-component rise of $[Ca^{2+}]_i$ in the native system. However, because COS-7 and HEK-293 do not express GPR40, this clearly rules out a requirement for GPR40 activation in oleate-induced potentiation of LTCC Ca^{2+} currents, even if the precise mechanism(s) remains to be clarified. The potentiation that we observed did not appear to require calcium influx, because a similar degree of potentiation was observed when calcium was replaced by barium in the extracellular solution. This work also does not elucidate whether the Ca^{2+} channel itself or another protein in intimate association with the channel is the direct target of fatty acids or their LC-CoA derivatives. Our use of triacsin C, which as a specific inhibitor of acyl-CoA synthetases blocks the first step in intracellular utilization of fatty acids, suggests that the oleoyl- CoA and not oleate itself may be required for potentiation to occur.

ACKNOWLEDGMENTS

We thank E. Perez-Reyes for providing the rat brain β-isoforms and P. O. Berggren for the rabbit lung α_{1C}- and rat islet β-isoforms. S. Tavalin provided technical advice on transfecting HEK cells, and R. Bertram and S. Tavalin provided helpful input on the manuscript.

GRANTS

This work was supported by National Institute of Diabetes and Digestive and Kidney Diseases Grants DK-63247 to L. Moitoso de Vargas and DK-46409 to L. S. Satin.

REFERENCES

1. Alcázar O, Qiu-yue Z, Giné E, Tamarit-Rodriguez J. Stimulation of islet protein kinase C translocation by palmitate requires metabolism of the fatty acid. Diabetes 1997;46:1153–1158. [PubMed: 9200650]

2. Atwater, I.; Carrol, P.; Li, MX. Electrophysiology of the pancreatic beta-cell. In: Draznin, B.; Melmed, S.; LeRoith, D., editors. Molecular and Cellular Biology of Diabetes Mellitus. New York: Liss; 1989. p. 49-68.
3. Barg S, Olofsson CS, Schriever-Abeln J, Wendt A, Gebre-Medhin S, Renstrom E, Rorsman P. Delay between fusion pore opening and peptide release from large dense-core vesicles in neuroendocrine cells. Neuron 2002;33:287–299. [PubMed: 11804575]
4. Berggren PO, Yang SN, Murakami M, Efanov AM, Uhles S, Kohler M, Moede T, Fernstrom A, Appelskog IB, Aspinwall CA, Zaitsev SV, Larsson O, de Vargas LM, Fecher-Trost C, Weissgerber P, Ludwig A, Leibiger B, Juntti-Berggren L, Barker CJ, Gromada J, Freichel M, Leibiger IB, Flockerzi V. Removal of Ca2+ channel beta3 subunit enhances Ca2+ oscillation frequency and insulin exocytosis. Cell 2004;119:273–284. [PubMed: 15479643]
5. Biel M, Ruth P, Bosse E, Hullin R, Stuhmer W, Flockerzi V, Hofmann F. Primary structure and functional expression of a high voltage activated calcium channel from rabbit lung. FEBS Lett 1990;269:409–412. [PubMed: 2169433]
6. Boden G. Role of fatty acids in the pathogenesis of insulin resistance and NIDDM. Diabetes 1997;46:3–10. [PubMed: 8971073]
7. Boden G, Chen X, Iqbal N. Acute lowering of plasma fatty acids lowers basal insulin secretion in diabetic and nondiabetic subjects. Diabetes 1998;47:1609–1612. [PubMed: 9753299]
8. Boyd, AE.; Rajan, AS. Regulation of insulin release by calcium. In: Draznin, B.; Melmed, S.; LeRoith, D., editors. Molecular and Cellular Biology of Diabetes Mellitus. Insulin Secretion. New York: Liss; 1989. p. 93-105.
9. Briscoe CP, Tadayyon M, Andrews JL, Benson WG, Chambers JK, Eilert MM, Ellis C, Elshourbagy NA, Goetz AS, Minnick DT, Murdock PR, Sauls HR Jr, Shabon U, Spinage LD, Strum JC, Szekeres PG, Tan KB, Way JM, Ignar DM, Wilson S, Muir AI. The orphan G protein-coupled receptor GPR40 is activated by medium and long chain fatty acids. J Biol Chem 2003;278:11303–11311. [PubMed: 12496284]
10. Brown AJ, Goldsworthy SM, Barnes AA, Eilert MM, Tcheang L, Daniels D, Muir AI, Wigglesworth MJ, Kinghorn I, Fraser NJ, Pike NB, Strum JC, Steplewski KM, Murdock PR, Holder JC, Marshall FH, Szekeres PG, Wilson S, Ignar DM, Foord SM, Wise A, Dowell SJ. The orphan G protein-coupled receptors GPR41 and GPR43 are activated by propionate and other short chain carboxylic acids. J Biol Chem 2003;278:11312–11319. [PubMed: 12496283]
11. Campillo JE, Valdivia MM, Rodriguez E, Osorio C. Effect of oleic and octanoic acids on glucose-induced insulin release in vitro. Diabetes Metab 1979;5:183–187.
12. Charles MA, Eschwege E, Thibult N, Claude JR, Warnet JM, Rosselin GE, Girard J, Balkau B. The role of non-esterified fatty acids in the deterioration of glucose tolerance in Caucasian subjects: results of the Paris Prospective Study. Diabetologia 1997;40:1101–1106. [PubMed: 9300248]
13. Chien AJ, Gao T, Perez-Reyes E, Hosey MM. Membrane targeting of L-type calcium channels. Role of palmitoylation in the subcellular localization of the beta2a subunit. J Biol Chem 1998;273:23590–23597. [PubMed: 9722599]
14. Coleman RA, Lewin TM, Van Horn CG, Gonzalez-Baró MR. Do long-chain acyl-CoA synthetases regulate fatty acid entry into synthetic versus degradative pathways? J Nutr 2002;132:2123–2126. [PubMed: 12163649]
15. Corkey BE, Glennon MC, Chen KS, Deeney JT, Matschinsky FM, Prentki M. A role for malonyl-CoA in glucose-stimulated insulin secretion from clonal pancreatic beta-cells. J Biol Chem 1989;264:21608–21612. [PubMed: 2689441]
16. Davalli AM, Biancardi E, Pollo A, Socci C, Pontiroli AE, Pozza G, Clementi F, Sher E, Carbone E. Dihydropyridine-sensitive and -insensitive voltage-operated calcium channels participate in the control of glucose-induced insulin release from human pancreatic beta cells. J Endocrinol 1996;150:195–203. [PubMed: 8869586]
17. de Vargas LM, Sobolewski J, Siegel R, Moss LG. Individual beta cells within the intact islet differentially respond to glucose. J Biol Chem 1997;272:26573–26577. [PubMed: 9334237]
18. Deeney JT, Prentki M, Corkey BE. Metabolic control of beta-cell function. Semin Cell Dev Biol 2000;11:267–275. [PubMed: 10966860]

19. DeFronzo RA, Ferrannini E. Insulin resistance. A multifaceted syndrome responsible for NIDDM, obesity, hypertension, dyslipidemia, and atherosclerotic cardiovascular disease. Diabetes Care 1991;14:173–194. [PubMed: 2044434]
20. Ford ES, Williamson DF, Liu S. Weight change and diabetes incidence: findings from a national cohort of US adults. Am J Epidemiol 1997;146:214–222. [PubMed: 9247005]
21. Fraze E, Donner CC, Swislocki AL, Chiou YA, Chen YD, Reaven GM. Ambient plasma free fatty acid concentrations in noninsulin-dependent diabetes mellitus: evidence for insulin resistance. J Clin Endocrinol Metab 1985;61:807–811. [PubMed: 3900120]
22. Fujimoto WY, Bergstrom RW, Boyko EJ, Chen K, Kahn SE, Leonetti DL, McNeely MJ, Newell LL, Shofer JB, Wahl PW. Type 2 diabetes and the metabolic syndrome in Japanese Americans. Diabetes Res Clin Pract 2000;50:S73–S76. [PubMed: 11024587]
23. Fujiwara K, Maekawa F, Yada T. Oleic acid interacts with GPR40 to induce Ca^{2+} signaling in rat islet β-cells: mediation by PLC and L-type Ca^{2+}channel and link to insulin release. Am J Physiol Endocrinol Metab 2005;289:E670–E677. [PubMed: 15914509]
24. Gao T, Chien AJ, Hosey MM. Complexes of the alpha1C and beta subunits generate the necessary signal for membrane targeting of class C L-type calcium channels. J Biol Chem 1999;274:2137–2144. [PubMed: 9890976]
25. Grynkiewicz G, Poenie M, Tsien RY. A new generation of Ca2+ indicators with greatly improved fluorescence properties. J Biol Chem 1985;260:3440–3450. [PubMed: 3838314]
26. Hamilton JA, Kamp F. How are free fatty acids transported in membranes? Is it by proteins or by free diffusion through the lipids? Diabetes 1999;48:2255–2269. [PubMed: 10580412]
27. Heart E, Corkey RF, Wikstrom JD, Shirihai OS, Corkey BE. Glucose-dependent increase in mitochondrial membrane potential, but not cyto-plasmic calcium, correlates with insulin secretion in single islet cells. Am J Physiol Endocrinol Metab 2006;290:E143–E148. [PubMed: 16144817]
28. Hirasawa A, Tsumaya K, Awaji T, Katsuma S, Adachi T, Yamada M, Sugimoto Y, Miyazaki S, Tsujimoto G. Free fatty acids regulate gut incretin glucagon-like peptide-1 secretion through GPR120. Nat Med 2005;11:90–94. [PubMed: 15619630]
29. Hurley JH, Cahill AL, Currie KP, Fox AP. The role of dynamic palmitoylation in Ca2+ channel inactivation. Proc Natl Acad Sci USA 2000;97:9293–9298. [PubMed: 10900273]
30. Igal RA, Wang P, Coleman RA. Triacsin C blocks de novo synthesis of glycerolipids and cholesterol esters but not recycling of fatty acid into phospholipid: evidence for functionally separate pools of acyl-CoA. Biochem J 1997;324:529–534. [PubMed: 9182714]
31. Ihara Y, Yamada Y, Fujii Y, Gonoi T, Yano H, Yasuda K, Inagaki N, Seino Y, Seino S. Molecular diversity and functional characterization of voltage-dependent calcium channels (CACN4) expressed in pancreatic beta-cells. Mol Endocrinol 1995;9:121–130. [PubMed: 7760845]
32. Iwashima Y, Pugh W, Depaoli AM, Takeda J, Seino S, Bell GI, Polonsky KS. Expression of calcium channel mRNAs in rat pancreatic islets and downregulation after glucose infusion. Diabetes 1993;42:948–955. [PubMed: 7685720]
33. Kinard TA, Satin LS. An ATP-sensitive Cl_- channel current that is activated by cell swelling, cAMP, and glyburide in insulin-secreting cells. Diabetes 1995;44:1461–1466. [PubMed: 7589855]
34. Koyama K, Chen G, Lee Y, Unger RH. Tissue triglycerides, insulin resistance, and insulin production: implications for hyperinsulinemia of obesity. Am J Physiol Endocrinol Metab 1997;273:E708–E713.
35. Le Poul E, Loison C, Struyf S, Springael JY, Lannoy V, Decobecq ME, Brezillon S, Dupriez V, Vassart G, Van Damme J, Parmentier M, Detheux M. Functional characterization of human receptors for short chain fatty acids and their role in polymorphonuclear cell activation. J Biol Chem 2003;278:25481–25489. [PubMed: 12711604]
36. Magnelli V, Pollo A, Sher E, Carbone E. Block of non-L-, non-N-type Ca2+ channels in rat insulinoma RINm5F cells by omega-agatoxin IVA and omega-conotoxin MVIIC. Pflugers Arch 1995;429:762–771. [PubMed: 7603830]
37. Massa E, Kelly KM, Yule DI, MacDonald RL, Uhler MD. Comparison of fura-2 imaging and electrophysiological analysis of murine calcium channel alpha 1 subunits coexpressed with novel beta 2 subunit isoforms. Mol Pharmacol 1995;47:707–716. [PubMed: 7723731]

38. McLaughlin JT, Lomax RB, Hall L, Dockray GJ, Thompson DG, Warhurst G. Fatty acids stimulate cholecystokinin secretion via an acyl chain length-specific, Ca2+-dependent mechanism in the enteroendocrine cell line STC-1. J Physiol 1998;513:11–18. [PubMed: 9782155]
39. Mokdad AH, Bowman BA, Ford ES, Vinicor F, Marks JS, Koplan JP. The continuing epidemics of obesity and diabetes in the United States. JAMA 2001;286:1195–1200. [PubMed: 11559264]
40. Ohta M, Nelson J, Nelson D, Meglasson MD, Erecinska M. Effect of Ca+ + channel blockers on energy level and stimulated insulin secretion in isolated rat islets of Langerhans. J Pharmacol Exp Ther 1993;264:35–40. [PubMed: 8423537]
41. Olcese R, Qin N, Schneider T, Neely A, Wei X, Stefani E, Birnbaumer L. The amino terminus of a calcium channel beta subunit sets rates of channel inactivation independently of the subunit's effect on activation. Neuron 1994;13:1433–1438. [PubMed: 7993634]
42. Olofsson CS, Salehi A, Gopel SO, Holm C, Rorsman P. Palmitate stimulation of glucagon secretion in mouse pancreatic alpha-cells results from activation of L-type calcium channels and elevation of cytoplasmic calcium. Diabetes 2004;53:2836–2843. [PubMed: 15504963]
43. Olofsson CS, Salehi A, Holm C, Rorsman P. Palmitate increases L-type Ca2+ currents and the size of the readily releasable granule pool in mouse pancreatic beta-cells. J Physiol 2004;557:935–948. [PubMed: 15090611]
44. Perez-Reyes E, Wei XY, Castellano A, Birnbaumer L. Molecular diversity of L-type calcium channels. Evidence for alternative splicing of the transcripts of three nonallelic genes. J Biol Chem 1990;265:20430–20436. [PubMed: 2173707]
45. Plant TD. Properties and calcium-dependent inactivation of calcium currents in cultured mouse pancreatic B-cells. J Physiol 1988;404:731–747. [PubMed: 2855352]
46. Prentki M. New insights into pancreatic beta-cell metabolic signaling in insulin secretion. Eur J Endocrinol 1996;134:272–286. [PubMed: 8616523]
47. Prentki M, Corkey BE. Are the beta-cell signaling molecules malonyl-CoA and cystolic long-chain acyl-CoA implicated in multiple tissue defects of obesity and NIDDM? Diabetes 1996;45:273–283. [PubMed: 8593930]
48. Prentki M, Vischer S, Glennon MC, Regazzi R, Deeney JT, Corkey BE. Malonyl-CoA and long chain acyl-CoA esters as metabolic coupling factors in nutrient-induced insulin secretion. J Biol Chem 1992;267:5802–5810. [PubMed: 1556096]
49. Qin N, Platano D, Olcese R, Costantin JL, Stefani E, Birnbaumer L. Unique regulatory properties of the type 2a Ca2+ channel beta subunit caused by palmitoylation. Proc Natl Acad Sci USA 1998;95:4690–4695. [PubMed: 9539800]
50. Remizov O, Jakubov R, Düfer M, Krippeit Drews P, Drews G, Waring M, Brabant G, Wienbergen A, Rustenbeck I, Schöfl C. Palmitate-induced Ca2+-signaling in pancreatic beta-cells. Mol Cell Endocrinol 2003;212:1–9. [PubMed: 14654245]
51. Resnick HE, Valsania P, Halter JB, Lin X. Relation of weight gain and weight loss on subsequent diabetes risk in overweight adults. J Epidemiol Community Health 2000;54:596–602. [PubMed: 10890871]
52. Richieri GV, Anel A, Kleinfeld AM. Interactions of long-chain fatty acids and albumin: determination of free fatty acid levels using the fluorescent probe ADIFAB. Biochemistry 1993;32:7574–7580. [PubMed: 8338853]
53. Roden M, Price TB, Perseghin G, Petersen KF, Rothman DL, Cline GW, Shulman GI. Mechanism of free fatty acid-induced insulin resistance in humans. J Clin Invest 1996;97:2859–2865. [PubMed: 8675698]
54. Roduit R, Nolan C, Alarcon C, Moore P, Barbeau A, Delghingaro-Augusto V, Przybykowski E, Morin J, Masse F, Massie B, Ruderman N, Rhodes C, Poitout V, Prentki M. A role for the malonyl-CoA/long-chain acyl-CoA pathway of lipid signaling in the regulation of insulin secretion in response to both fuel and nonfuel stimuli. Diabetes 2004;53:1007–1019. [PubMed: 15047616]
55. Rorsman P, Ashcroft FM, Trube G. Single Ca channel currents in mouse pancreatic B-cells. Pflugers Arch 1988;412:597–603. [PubMed: 2463514]
56. Rorsman P, Trube G. Calcium and delayed potassium currents in mouse pancreatic beta-cells under voltage-clamp conditions. J Physiol 1986;374:531–550. [PubMed: 2427706]

57. Santomauro AT, Boden G, Silva ME, Rocha DM, Santos RF, Ursich MJ, Strassmann PG, Wajchenberg BL. Overnight lowering of free fatty acids with Acipimox improves insulin resistance and glucose tolerance in obese diabetic and nondiabetic subjects. Diabetes 1999;48:1836–1841. [PubMed: 10480616]
58. Satin LS, Tavalin SJ, Kinard TA, Teague J. Contribution of L- and non-Ltype calcium channels to voltage-gated calcium current and glucosedependent insulin secretion in HIT-T15 cells. Endocrinology 1995;136:4589–4601. [PubMed: 7545106]
59. Shapiro H, Shachar S, Sekler I, Hershfinkel M, Walker MD. Role of GPR40 in fatty acid action on the beta cell line INS-1E. Biochem Biophys Res Commun 2005;335:97–104. [PubMed: 16081037]
60. Sidhu SS, Thompson DG, Warhurst G, Case RM, Benson RS. Fatty acid-induced cholecystokinin secretion and changes in intracellular Ca^{2+} in two enteroendocrine cell lines, STC-1 and GLUTag. J Physiol 2000;528:165–176. [PubMed: 11018115]
61. Spector AA, Hoak JC. Letter: fatty acids, platelets, and microcirculatory obstruction. Science 1975;190:490–492. [PubMed: 1166323]
62. Stein DT, Stevenson BE, Chester MW, Basit M, Daniels MB, Turley SD, McGarry JD. The insulinotropic potency of fatty acids is influenced profoundly by their chain length and degree of saturation. J Clin Invest 1997;100:398–403. [PubMed: 9218517]
63. Wang X, Zeng W, Murakawa M, Freeman MW, Seed B. Episomal segregation of the adenovirus enhancer sequence by conditional genome rearrangement abrogates late viral gene expression. J Virol 2000;74:11296–11303. [PubMed: 11070029]
64. Warnotte C, Gilon P, Nenquin M, Henquin JC. Mechanisms of the stimulation of insulin release by saturated fatty acids. A study of palmitate effects in mouse beta-cells. Diabetes 1994;43:703–711. [PubMed: 8168648]
65. Wilde DW, Massey KD, Walker GK, Vollmer A, Grekin RJ. High-fat diet elevates blood pressure and cerebrovascular muscle Ca(2+) current. Hypertension 2000;35:832–837. [PubMed: 10720603]
66. Wollheim CB, Sharp GW. Regulation of insulin release by calcium. Physiol Rev 1981;61:914–973. [PubMed: 6117094]
67. Xu W, Lipscombe. Neuronal Ca(V)1.3alpha(1) L-type channels activate at relatively hyperpolarized membrane potentials and are incompletely inhibited by dihydropyridines. J Neurosci 2001;21:5944–5951. [PubMed: 11487617]
68. Yamada Y, Masuda K, Li Q, Ihara Y, Kubota A, Miura T, Nakamura K, Fujii Y, Seino S, Seino Y. The structures of the human calcium channel alpha 1 subunit (CACNL1A2) and beta subunit (CACNLB3) genes. Genomics 1995;27:312–319. [PubMed: 7557998]

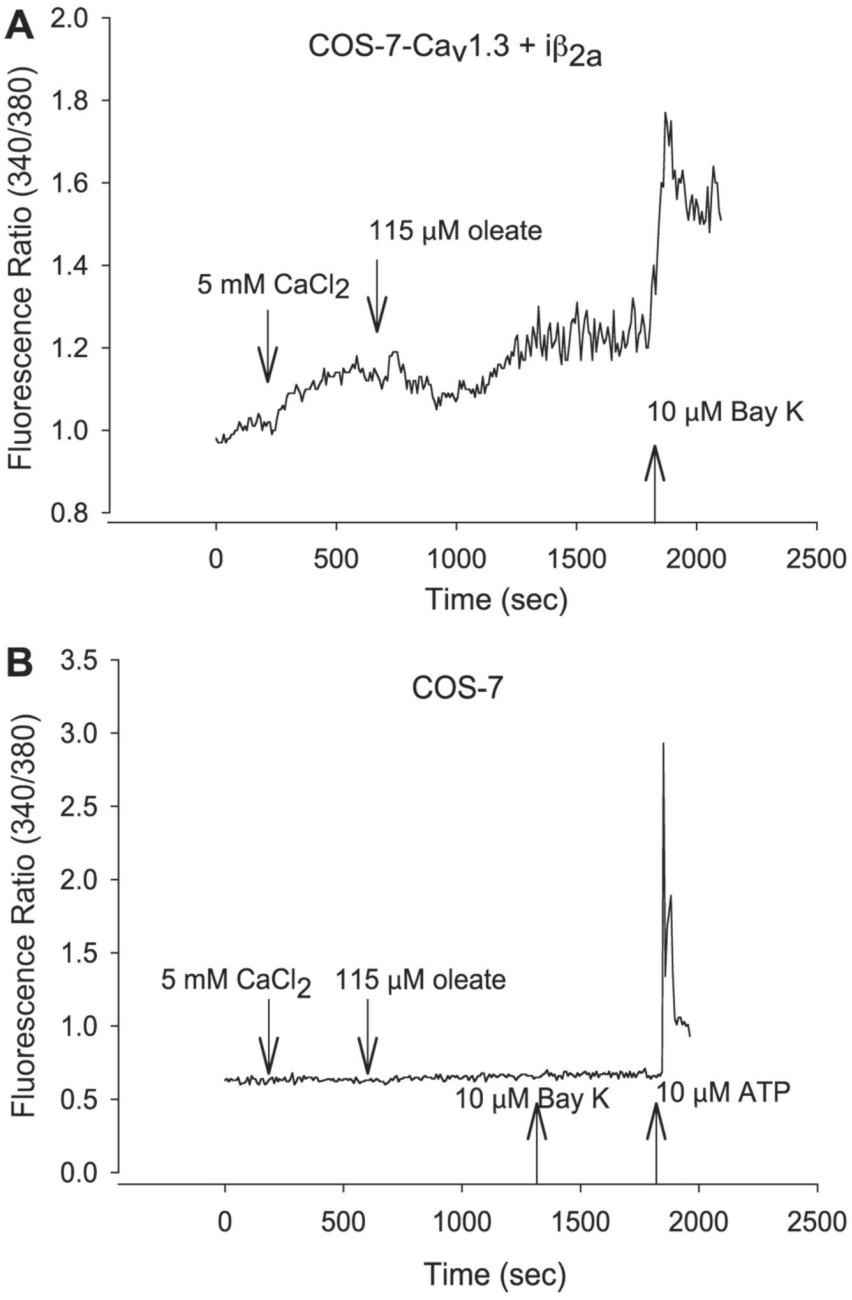

Fig. 1.

Oleate increases intracellular Ca^{2+} in single COS-7 cells expressing L-type voltage-dependent calcium channels (LTCC). Representative traces of changes in intracellular free calcium concentration ($[Ca^{2+}]_i$) in fura 2-loaded COS-7 cells as specified in MATERIALS AND METHODS in the presence of 10 mM glucose, 2 mM $CaCl_2$, and 0.05% BSA. Reagents were added sequentially at the times indicated as 500 μl bolus to the dish with a starting volume of 1 ml. *A*: COS-7 cells expressing Cav1.3-iβ_{2a} for 48-h posttransfer of transgenes. *B*: COS-7 control cells in the absence of any heterologous expression of transgenes.

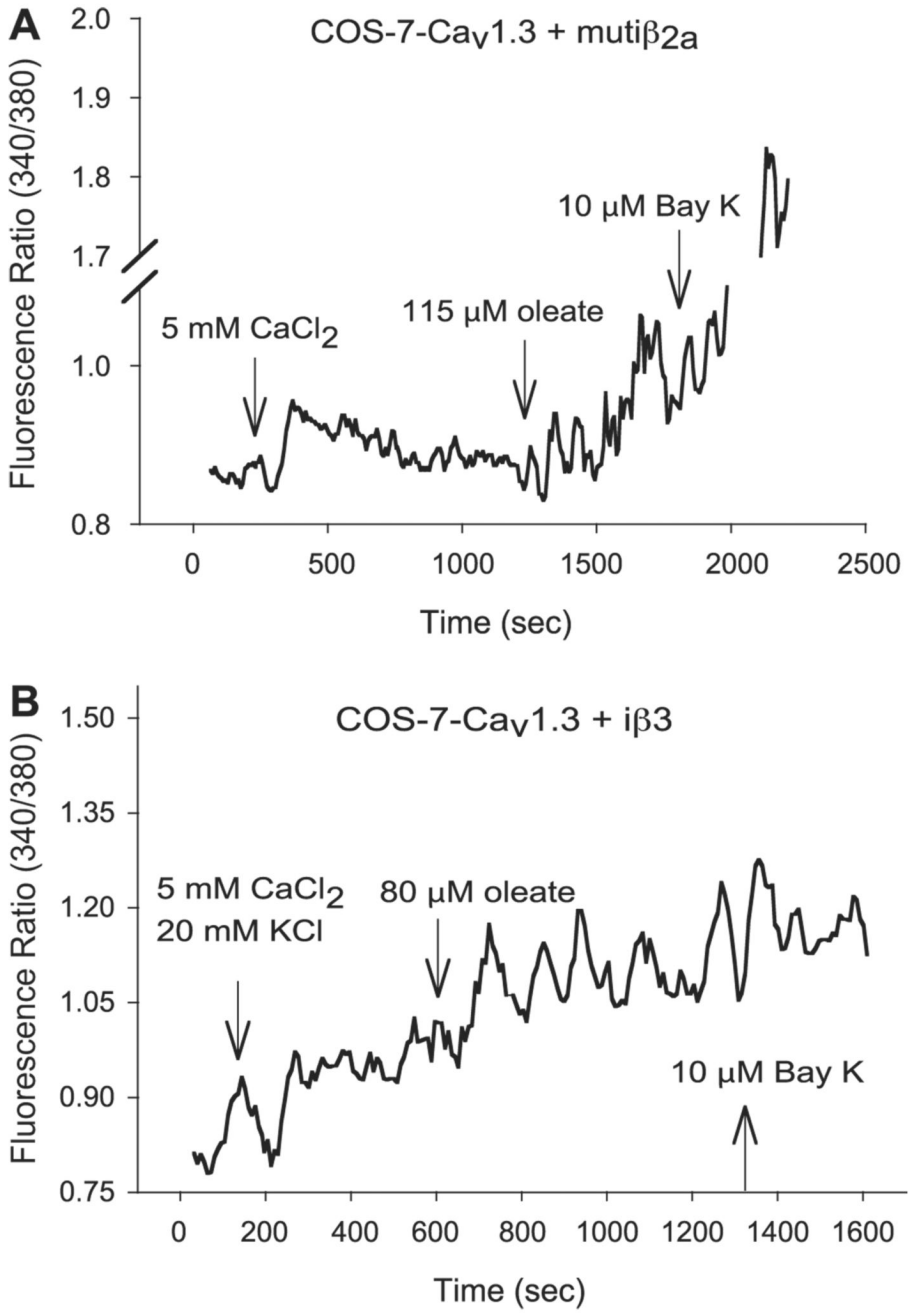

Fig. 2.

Oleate increases intracellular Ca^{2+} in single COS-7 cells expressing Cav1.3 plus mut $i\beta_{2a}$ or $i\beta_3$. Representative traces, generated with 5-point moving average, of fura 2-loaded COS-7 cells expressing Cav1.3-mut $i\beta_{2a}$ (*A*) and Cav1.3-$i\beta_3$ (*B*) imaged 48 h posttransgenes' transfer in the presence of 10 mM glucose, 2 mM $CaCl_2$, and 0.05% BSA and monitored for $[Ca^{2+}]_i$ changes after addition of 500 μl bolus of each reagent at the ndicated times.

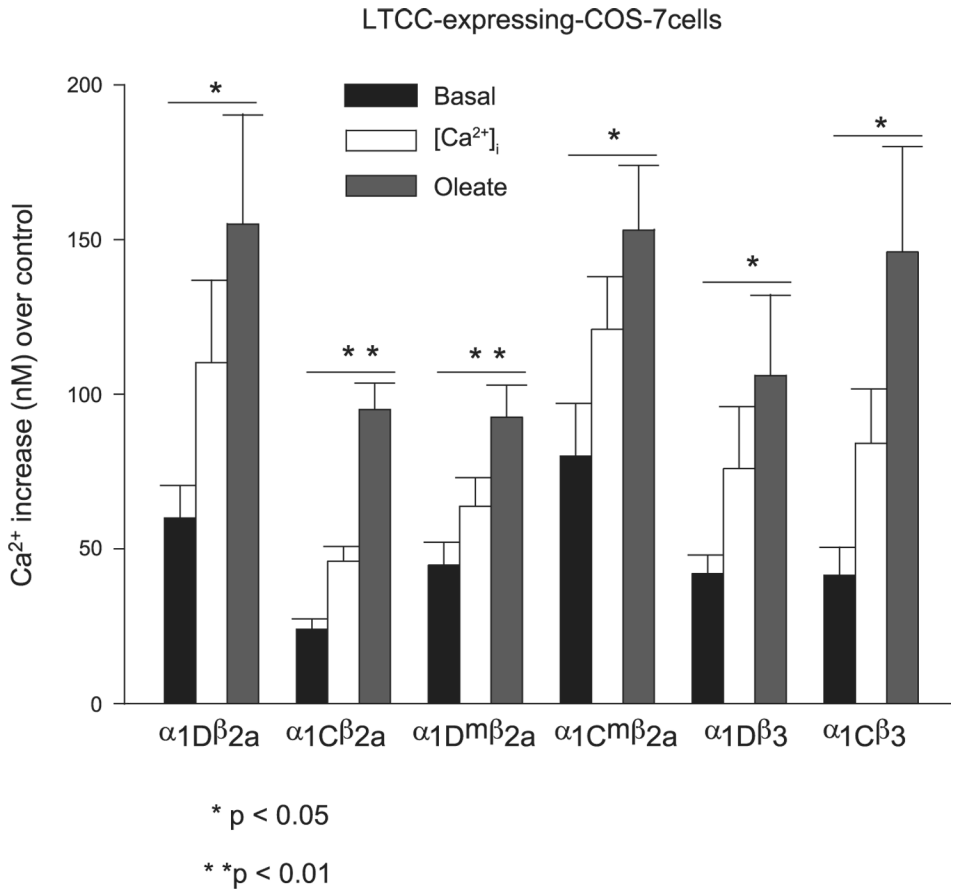

Fig. 3.

Mean oleate-induced increase in intracellular $[Ca^{2+}]_i$ in LTCC-expressing COS-7 cells. Intracellular free $[Ca^{2+}]_i$ increases for each condition were calculated from the fluorescent ratio for each parameter after subtraction of the equivalent value from control cells. A K_d of 224 nm/l for $[Ca^{2+}]_i$ binding to free fura-2 was used in the calculations. Data are means ± SE from ≥8 single cells and *P* values calculated using Student's paired *t*-test.

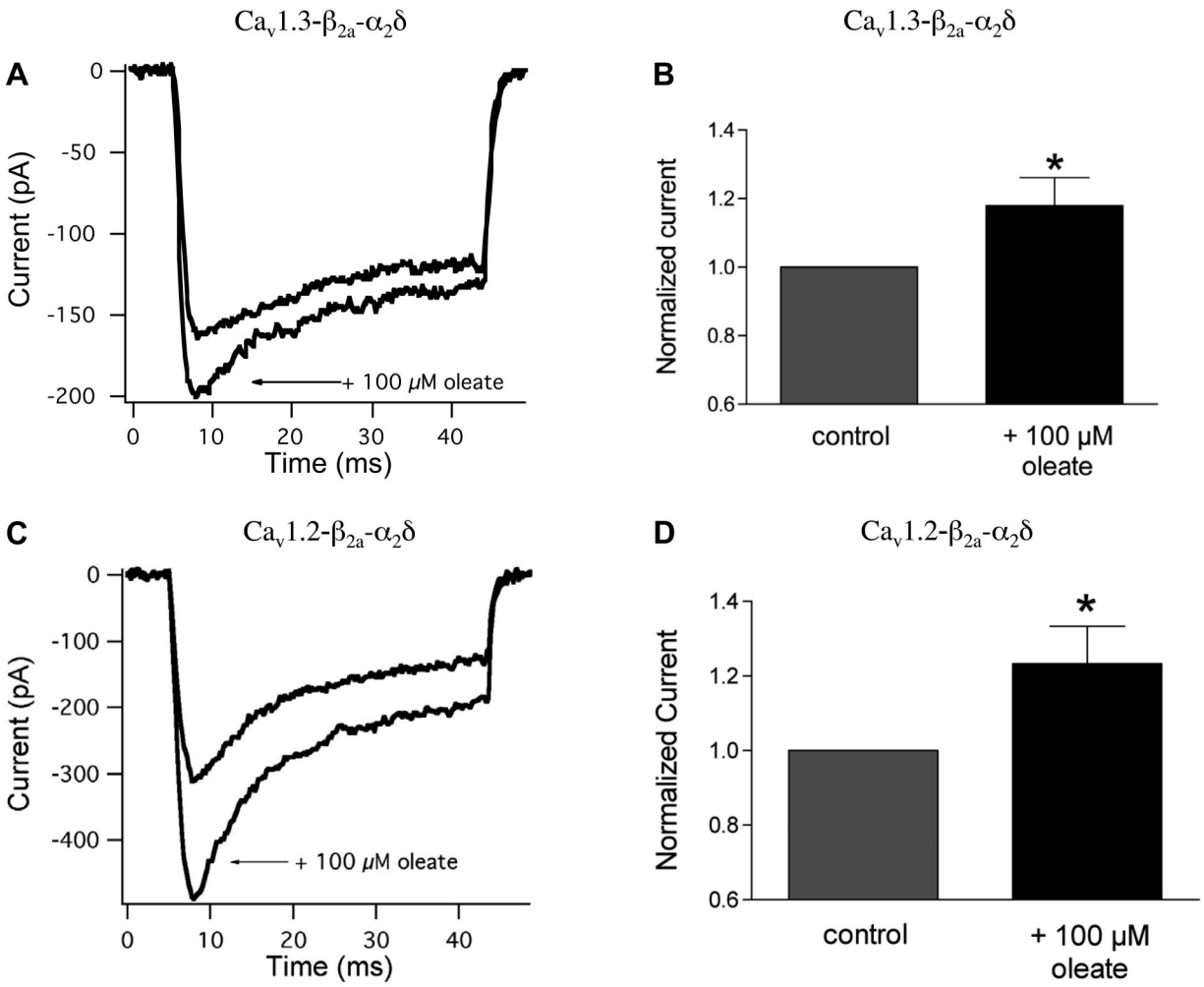

Fig. 4.

Oleate potentiates voltage-sensitive calcium current in HEK-293 cells expressing the calcium channel subunits Cav1.3 or Cav1.2 plus iβ_{2a} and β_2. *A*: representative whole cell calcium current traces recorded from HEK-293 cells expressing the calcium channel subunits Cav1.3-iβ_{2a}-$\beta_2\delta$. Currents were elicited by a voltage step from −65 to 0 mV in the presence and absence of 100 μM oleate. *B*: peak calcium current measured at 0 mV in the presence of oleate was normalized to the peak current measured in the absence of oleate. Application of 100 μM oleate increased mean calcium current amplitude at 0 mV by 18.1 ± 8.3% compared with control (n = 17, $P < 0.05$). *C*: representative whole cell calcium current traces recorded from HEK-293 cells expressing the calcium channel subunits Cav1.2-iβ_{2a}-$\alpha_2\delta$ in response to a voltage step from −65 to 0 mV. *D*: application of 100 μM oleate increased mean calcium current amplitude at 0 mV by 23.3 ± 10.0% compared with control (n = 24, $P < 0.05$).

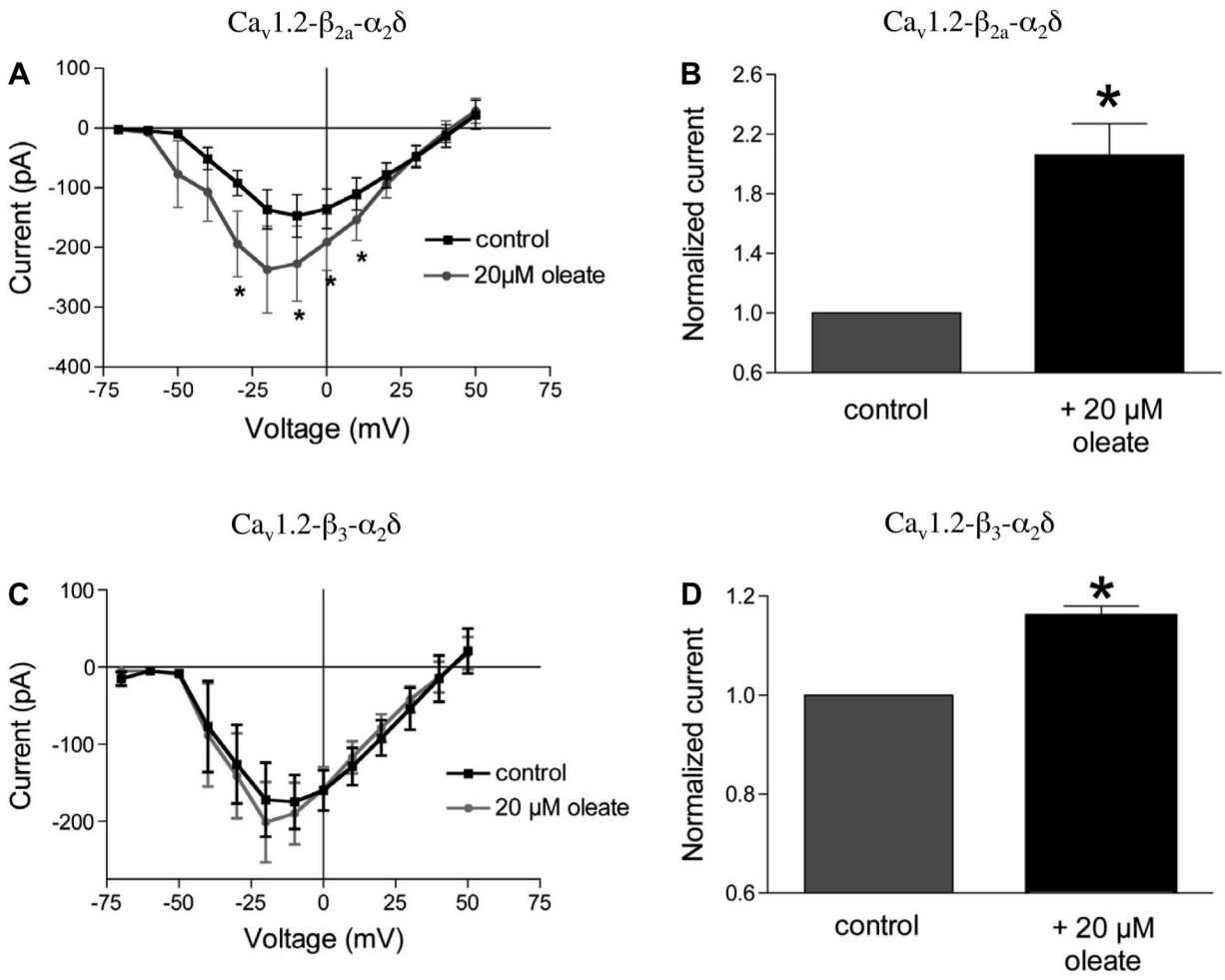

Fig. 5.

The expression of different β-subunit isoforms modulates the extent of oleate current potentiation. *A*: peak calcium currents were measured at voltages ranging from −70 to −50 mV in HEK-293 cells expressing the calcium channel subunits Cav1.2-iβ_{2a}-$\alpha_2\delta$ Current-voltage (I–V) curves are shown for peak currents measured in the presence (gray circles) and absence (■) of 20 μM oleate. *B*: mean normalized calcium current amplitude at 0 mV was plotted for currents measured in the presence and absence of oleate. Application of 20 μM oleate increased current amplitude by 106 ± 21% compared with control (n = 9, P < 0.002). C: I–V curves are shown for peak currents measured at voltages ranging from −70 to −50 mV in HEK-293 cells transfected with the calcium channel subunits Cav1.2-iβ_3-$\alpha_2\delta$ in the presence (gray circles) and absence (■) of 20 μM oleate. *D*: application of 20 μM oleate increased mean calcium current amplitude at 0 mV by 16 ± 2% compared with control (n = 8, P < 0.01).

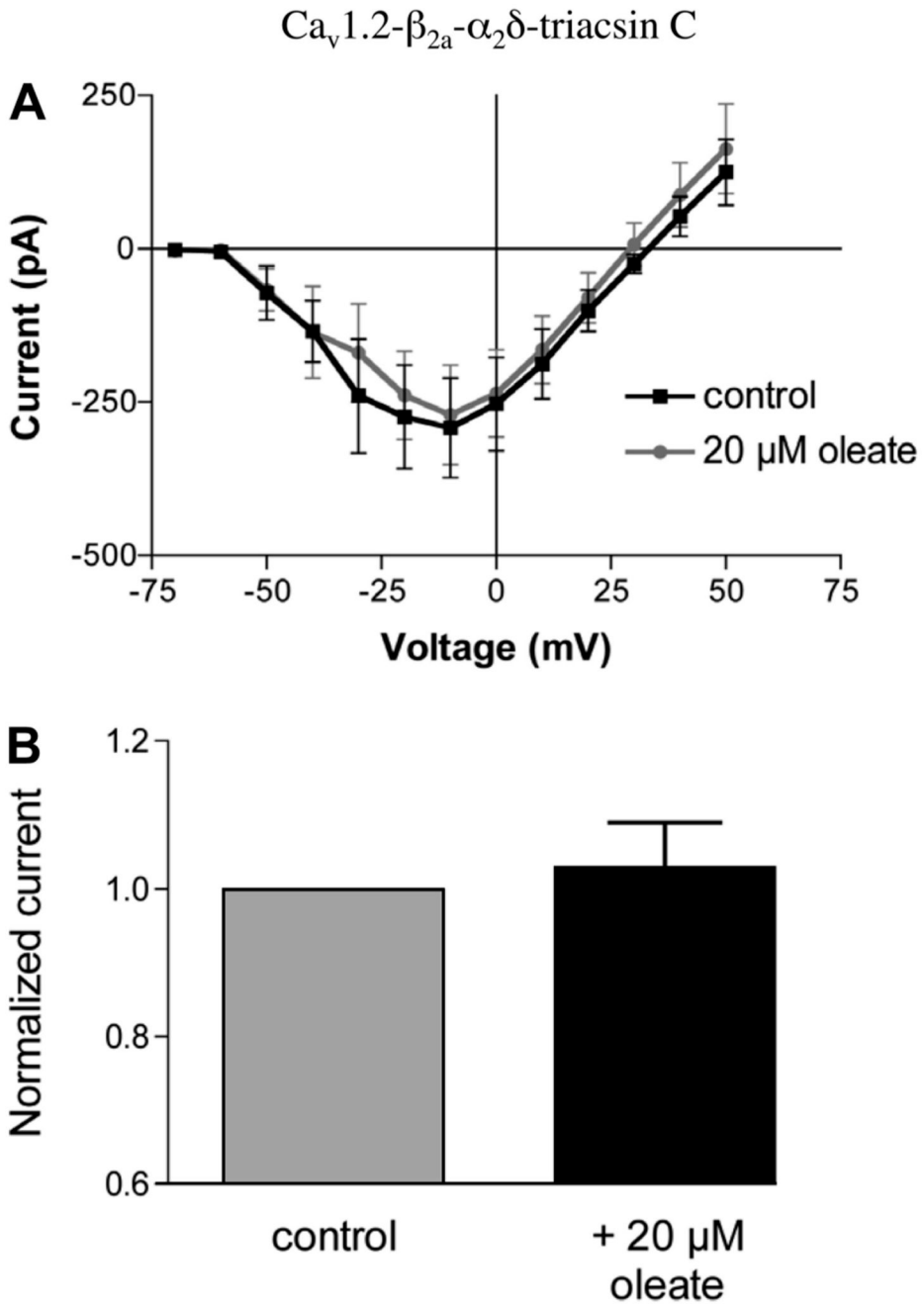

Fig. 6.

Triacsin C abolishes calcium current potentiation by oleate. *A*: HEK-293 cells expressing the calcium channel subunits Cav1.2-iβ_{2a}-α2δ were treated with 96 μM triacsin C for 20 min. Peak calcium currents were then measured at voltages ranging from −70 to −50 mV in the presence (gray circles) or absence (■) of 20 μM oleate. *B*: mean calcium current amplitude measured at 0 mV in the presence of oleate was normalized to control mean current amplitude without oleate. Application of 20 μM oleate did not significantly alter mean calcium current amplitude in triacsin C-treated cells ($n = 9$, $P > 0.05$).